FABRICATION OF TERNARY METAL SULFIDE QUANTUM DOTS LOADED ON MOLECULAR SIEVES AS A PHOTOCATALYST

AFSHIN POURAHMAD

Department of Chemistry, Rasht Branch, Islamic Azad University, Iran
Email: pourahmad@iaurasht.ac.ir

Abstract - The synthesis of ZnCdS nanomaterial in MCM-41 matrix has been realized by chemical synthesis between MCM-41, $ZnCl_2$ and $CdCl_2$ via an ion exchange method in aqueous solution. X-ray diffraction analysis (XRD), diffuse reflectance spectroscopy (DRS), transmission electron microscopy (TEM) and fourier transform infrared (FT-IR) were used to characterize the products. Several parameters were examined, catalyst amount (0.1-6 g L^{-1}), pH (3-12) and initial concentration of MB (0.16-3.2 ppm). The extent of degradation was estimated from the residual concentration by spectrophotometrically. The average size of ZnCdCl2 in MCM-41 nanostructure was obtained about 3 nm by TEM.

Keywords - Nanocomposite, Nanocatalyst, Methylene blue, Water Treatment, X-ray diffraction, Infrared spectroscopy.

I. INTRODUCTION

Recently, water shortages are becoming an increasing problem due to scientific advances following rapid industrial growth, environmental pollution, depleted water resources, global warming causing abnormal climate changes, and uncontrolled groundwater development [1]. The rapid development of manufacturing technology after the industrial revolution has improved the standards of living significantly but it is becoming a factor that is threatening human health and the environment. Pollutants are changing both quantitatively and qualitatively, and the number of chemicals currently in circulation is 38,000 with more than 300 new materials being synthesized every year due to the diversification of industrial structures and high-tech industry [2]. In line with national development, growth and policy, industrial wastewater is becoming more contaminated and difficult to process. In particular, there are few effective and economic treatment methods for livestock manure and litter leachate. Organic compounds and toxic pesticides, and manure emission from each industry are polluting drinking water and rivers, which is becoming a worldwide contamination with increased severity. The wide area of water pollution, diversification and nonbiodegradable problems has become a problem that cannot be solved by the natural cleansing cycle [3]. One of the most important challenges for science is to develop efficient methods to control environmental pollution. The II–VI semiconductor systems have many applications, such as in catalysts, solar cells, electronic and optoelectronic nanodevices. Mesoporous silicates have attracted much attention in the field of separation, adsorption and catalysis due to their remarkable features such as high surface area, high pore volume, regular structure, uniform pore size distribution and high thermal stability [4]. In this work, we prepared ZnCdS quantum dots via an ion exchange route. The photocatalytic activity of the prepared samples was examined using photocatalytic degradation of methylene blu in water under UV light irradiation.

II. DETAILS EXPERIMENTAL

2.1. Materials

The $ZnCl_2$ and $CdCl_2$, from Merck, were used as source of metal ions and $Na_2S.\ 9H_2O$ (Merck) was used as source of sulfide ion. Hydrochloric acid and sodium hydroxide were applied for variation of pH of sample solutions. The dye of methylene blue (C.I. name: Basic Blue 9, $C_{16}H_{18}ClN_3S{:}3H_2O$) was purchased from Fluka company.

2.2. Preparation of molecular sieves nanoparticles

Nano-sized mesoporous MCM-41 silica with particle size ~ 90 nm was synthesized by a room temperature method with some modification to the procedure described in the literature [5]. We used tetraethylorthosilicate (TEOS: Merck, 800658) as a source of silicon and hexadecyltrimethylammonium bromide (HDTMABr; BOH, 103912) as a surfactant template for preparation of the mesoporous material. The molar composition of the reactant mixture is as fallows:

TEOS: 0.31NaOH: 0.125HDTMABr: $1197H_2O$

The prepared nano-sized MCM-41 was calcined at 550 °C for 5h to decompose the surfactant and obtain the white powder. Surfactant-free MCM-41 nanoparticles were used for loading the zinc sulfide nanoparticles.

2.3. Preparation of ZnCdS/MCM-41 anocomposite

Two solutions, 0.1 M of $ZnCl_2$ and $CdCl_2$, were prepared as precursors of the ZnS and CdS semiconductors. For each ion exchange, 1 g of MCM-41 powder was added to different mixtures of the precursors, as illustrated in Table 1, maintaining the total solution volume constant at 50 mL and stirred at room temperature for 12 h. After that, the

samples were washed to remove unexchanged Zn and Cd ions and air- dried. Finally, sulphirizing of the Zn and Cd ions was carried out with 0.1 M Na_2S solution. To make the reaction with the S^{2-} ion, 1 g of Zn^{2+} - Cd^{2+} - exchanged molecular sieve was added to 50 mL of 0.1 M solution of Na_2S at a fixed temperature, and magnetically stirred for 2 h. The samples were washed with deionized water and collected by filtration. The obtained samples were fine yellow colored powders. The samples were stable at ambient conditions and their color did not change when exposed to the contact of atmospheric moisture.

Table 1. Sample identification by the mixture of starting solutions for ionic exchange.

Sample lable	Mixture of starting solutions
Zn40Cd10S/MCM-41	40 mL $ZnCl_2$ + 10 mL $CdCl_2$
Zn25Cd25S/MCM-41	25 mL $ZnCl_2$ + 25 mL $CdCl_2$
Zn10Cd40S/MCM-41	10 mL $ZnCl_2$ + 40 mL $CdCl_2$

2.4. Characterization

X-ray diffraction (XRD) pattern was recorded on a Seisert Argon 3003 PTC using nickel-filtered XD-3a CuKα radiations (λ = 1.5418 ºA). The UV-vis diffused reflectance spectra (UV-vis DRS) were obtained from UV-vis Scinco 4100 spectrometer with an integrating sphere reflectance accessory. $BaSO_4$ was used as a reference material. UV-vis absorption spectra were recorded using a Shimadzu 1600 pc in the spectral range of 190-900nm. Transmission electron microscopy (TEM) was performed on a Philips CM10 and microscope operated at 100 kV. Samples were prepared by dispersing the powder in ethanol. Imaging was enabled by depositing few drops of suspension on a carbon coated 400 mesh Cu grid. The solvent was left to evaporate before imaging. Scanning electron microscopy (SEM) images of fabricated ZnS nanoparticles were obtained using LEO 440i electron microscope. The specific surface area and pore volume of the samples were calculated according to the Brunauer-Emmett-Teller (BET) method. Infrared spectra on KBr pellet were measured on a Bruek spectrophotometer.

2.5. Procedures of photodegradation of methylene blue

Photodegrdation experiments were performed with a photocatalytic reactor system. This bench scale system consisted of cylindrical Pyrex glass cell with 1.0 L capacity, 10cm inside diameter and 15cm height. A UV lamp was placed in a 5 cm diameter quartz tube with one end tightly sealed by a Teflon stop the lamp and the tube were then immersed in the photoreactor cell with a light path of 3.0 cm. The photoreactor was filled with 25 ml of 0.16 - 3.2 ppm of dye as pollutant and 0.02-5.00 g/L of ZnCdS/MCM-41 as nanophotocatalyst. The whole reactor was cooled with a water cooled jacket on its outside and the temperature was kept at 25 ˚C .All reactants in the reactions were stirred using a magnetic stirrer to ensure that the suspension of the catalyst was uniform during the course of the reaction. To determine the percent of destruction of dyes, the samples were collected at regular intervals, and centrifuged to remove the nanocatalyst particles that exist as undissolved particles in the samples. The wavelengths absorbance maximum (λmax) of methylene blue is 664 nm. Therefore, photometric analysis of samples before and after of irradiation can be used for measurement of the %D (degradation efficiency of dye). The absorption of solution and solid samples was measured by a UV-vis spectro photometer shimadzu model 1600 PC and UV-vis diffused reflectance spectrometer UV-vis DRS Scinco model 4100, respectively. The decrease of absorbance value of samples at λmax of dye after irradiation in a certain time interval will be shown rate of decolorization and therefore, photodegradation efficiency of the dye as well as the activity of nanoparticles as photocatalyst. The decolorization and degradation efficiency have been calculated as:

$$\%D = 100 \times [C_o\text{-}C / C_o]$$

Where C_o is the initial concentration of dye and C is the concentration of dye after irradiation in selected time interval. In order to obtain maximum degradation efficiency, pH, concentration of dye and amount of photocatalyst were studied in amplitudes of 3-12, 0.16-3.2 ppm and 0.1-6 g/L respectively.

III. RESULTS AND DISCUSSION

3.1. Characterization of ZnCdS nanoparticles in molecular sieves nanoparticles

Fig. 1 shows the XRD patterns of MCM-41 nanoparticles template and ZnCdS loading on the template. Measurements of the samples were carried out in the 2θ different ranges (2θ = 2-10º and 2θ = 10-60º). Low angle X-ray diffraction patterns (2θ = 2-10º) of calcined MCM-41 and ZnCdS/MCM-41 clearly exhibit four well-defined peaks which can be indexed with (100), (110), (200), and (210) planes on hexagonal unit cell, indicating mesoporous structure of MCM-41. The peak appearing at low angle (2θ = 2.2) corresponds to (100) plane of MCM-41 indicating ordered pore structure of MCM-41, which can be attributed to quasi-two dimensional hexagonal lattice of MCM-41 [5]. In this figure, we observed that all X-ray patterns are very similar. However, some differences, such as the broadening and slight shifting to higher angles of the diffraction peaks as well as the decrease of their intensity can be observed in the spectra.

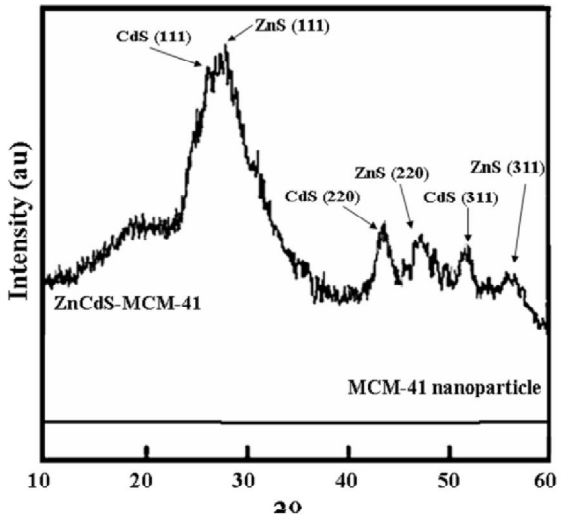


Fig. 1. X-ray diffraction patterns of MCM-41 nanoparticles and ZnCdS-MCM-41 in range 2θ = 10-60°.

This should be attributed to the porefilling effects that can reduce the scattering contrast between the pores and the framework MCM-41 materials. These decreases of the peak intensities, are in agreement with the reported results for other zeolites [6]. High angle X-ray diffraction pattern (2θ = 10-60), Fig. 1, further supports presence of ZnCdS. As we can see, the six peaks correspond to the face center cubic ZnS phase (111, 220, 311) and face center cubic CdS phase (111, 220, 311). The broadening of these peaks suggests the presence of small ZnS and CdS particles. These results reveal that the product is a nanocomposite consisting of ZnCdS phase. We have determined the size of nanoparticles at the mentioned 2θ by using the Debye-Scherrer formula, $d=0.9\ \lambda/\beta\cos\theta$, where d is the average diameter of the crystalline, λ the wavelength of X-ray, β the excess line width of the diffraction peak in radians and θ the Bragg angle. Based on this analysis the average size of ZnCdS quantum dots has been found 3 nm (Table 2).

The IR spectra of MCM-41 nanoparticles and ZnCdS/MCM-41 samples are recorded in the range of 400-4000 cm-1. The broad absorption band in the region 3765-3055 cm^{-1} can be attributed to the stretching of the framework Si-OH group with the defective sites and physically adsorbed water molecules. The vibrations of Si-O-Si can be seen at 1091 cm^{-1} (asymmetric stretching), 805 cm^{-1} (symmetric stretching) and 454 cm^{-1} (bending) [5]. In present work, all bands in ZnCdS-MCM-41 sample show shift to higher wave numbers with respect to the MCM-41 zeolite. This shift reveals that nanoparticles could incorporate in MCM-41 nanoparticles. The increased intensity is observed in ZnCdS/MCM-41 sample with respect to MCM-41 zeolite. This increased relates to extent of perturbation of T-O-T vibrations of the zeolite lattice (bands 400-1700 cm^{-1}) and increase in acidic bridged hydroxyls vibrations (3423 cm^{-1} band) [5]. These kind of differences are related to presence of ZnCdS quantum dots in MCM-41 nanoparticles.

Table 2. Band gap, specific surface area, particle size, pore volume and absorption edge of samples.

Sample	Band gap (eV)	Specific surface area (m^2/g)	Particle size (nm)	Pore volume (cc/g)	Absorption edge (nm)
-	1.05	90	850	-	MCM-41
375	-	-	-	3.6	ZnS
540	-	-	-	2.5	CdS
420	0.84	3	750	3.3	Zn40Cd10S/MCM-41
450	0.83	3	742	2.95	Zn25Cd25S/MCM-41
490	0.80	3	730	2.65	Zn10Cd40S/MCM-41

The specific surface area and pore volume of the MCM-41 nanoparticles and nanocomposites samples are presented in Table 2. As can be seen from Table 2, the pore volume of MCM-41 nanoparticle, which was 1.05 mL/g, decreased to 0.8-0.84 mL/g in ternary systems. Similarly, the specific surface areas of the nanocomposite materials were decreased from 850 $m^2\ g^{-1}$ for MCM-41 nanoparticles to 730-750 $m^2\ g^{-1}$ for ZnCdS/MCM-41. The decrease in the surface area and volumes of the pores of the MCM-41 in ternary systems has demonstrated that the guest can be located in the pores of MCM-41 mesopore molecular sieve.

Transmission electron microscopy along with the textural properties of the samples discussed above bring us important information regarding whether the ZnCdS particles are located inside or outside the pore structures used in this work. TEM image of ZnCdS/MCM-41 sample is shown in Fig. 2.

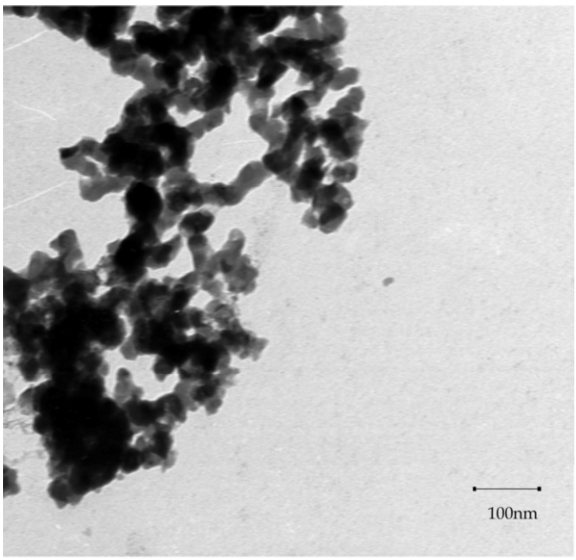


Fig. 2. Transmission electron microscopy (TEM) image of ZnCdS/MCM-41.

It was recorded under parallel direction to the pore axis and it is possible to observe typical MCM-41 morphology in the micrograph. Although it is very difficult to identify ZnCdS nanoparticles within the

pores of MCM-41 materials by using TEM t echniques [7], the higher contrast in the image of the ZnCdS/MCM-41 sample can be associated with the presence of ZnCdS nanoparticles inside the pores of this sample.

The UV-vis diffused reflectance spectra (UV-vis DRS) for ZnCdS nanoparticles prepared from MCM-41 matrices, bulk ZnS and bulk CdS shown in Fig. 3. The bulk ZnS and bulk CdS (Fig. 3) gave absorption below 400 nm and 600 nm, respectively. Comparing the absorption edge of bulk CdS to that of ZnCdS/MCM-41 samples prepared from mesoporous materials, it is seen that a blue shift in the onset of absorption has occurred in these samples. This blue shift indicates that ZnCdS exists as small clusters within the zeolite pores as reported by several researchers [8]. This was supported by a significant decrease in the surface area of ZnCdS/MCM-41, compared to the parent zeolite (Table 2). As can be seen, the samples show blue shifts in the absorption edge when the Cd concentration decreases and correspondingly the Zn concentration increases. This behavior is in agreement with that reported in previous works using the hydrothermal method and other studies where similar behavior in nanoparticles of the same semiconductors is observed. It can be noticed that the difference in optical behavior of the samples containing ZnCdS clusters is dominated by the presence of the Cd ions and not by the size of the nanoparticles. From the onset of the absorption edge, the band gap of the ZnCdS particles was calculated using the method of Tandon and Gupta (Table 2). The size of ZnCdS nanoparticles, estimated based on the results of Weller et al. was 3 nm for ZnCdS/MCM-41 samples.

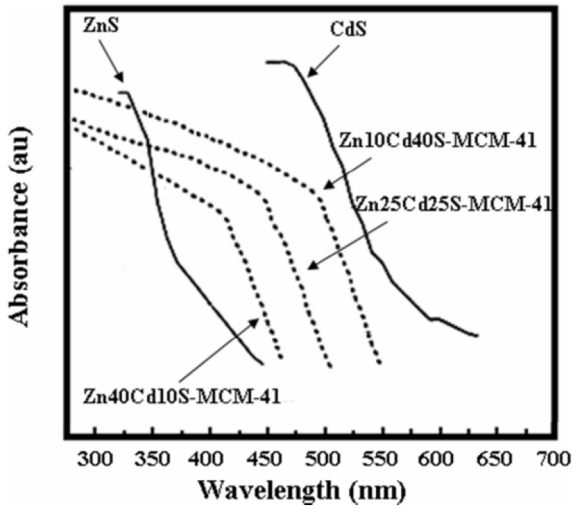


Fig. 3. UV-vis absorption spectrum of bulk ZnS, bulk CdS and ZnCdS-MCM-41.

3.2. Photodegradation of methylene blue using ZnCdS/MCM-41 nanocomposite

The time dependent electronic absorption spectrum of dye during photo irradiation was presented in Fig. 4. After 20 min of irradiation under UV light in a ZnCdS/MCM-41 suspension, 95% of dye was decomposed and decolorization of solution was observed. Besides, no new bands appear in the UV-vis region due to the reaction intermediates formed during the degradation process.

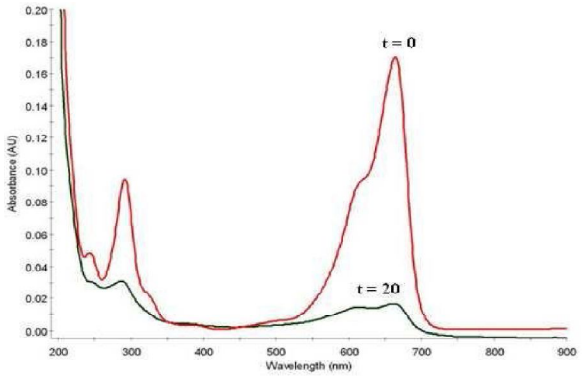


Fig. 4. Spectra change that occur during the photocatalytic degradation of aqueous solution of methylene blue: pH = 10, [20 wt% ZnCdS/MCM-41] = 0.4 g/L, Co = 0.32 ppm.

The effect of UV irradiation, ZnCdS, MCM-41 and ZnCdS/MCM-41 material on photodegradation of methylene blue are shown in Fig. 5. This figure indicates that in the presence of mixed photonanocatalyst and UV irradiation, 95% of dye degraded at the irradiation time of 20 min while it was 16% for MCM-41 and UV irradiation and 46.5% for ZnS (without MCM-41) at the irradiation time of 60 min. It is 3% degradation in the presence of UV light alone. These experiments demonstrated that both UV light and a photocatalyst, are needed for the effective degradation of dye. It is well documented that the absorption of photons possessing energy equal to or higher than that of the semiconductor (2.95 eV for ZnCdS in MCM-41) causes charge separation:

$$ZnCdS + hv \rightarrow ZnCdS(e^-) + ZnCdS(h^+)$$

The photogenerated holes may then react with adsorbed dye and oxidize the dye molecule by the formation of hydroxyl radicals. The photo-produced electrons in the conduction band react with the adsorbed oxygen to produced reactive radicals to yield the reactive oxygen species. To understand the role of support during the photocatalytic degradation of dye, the amount of ZnCdS nanoparticles available over 20 wt% ZnCdS supported system is considered for the degradation activity and the studies are carried out using 0.4 g/L catalyst in0.32 ppm methylene blue. From Figs. 4 and 5, it is observed that ZnCdS supported system is showing higher rate of degradation than ZnCdS or MCM-41 alone. This is due to the higher adsorption capacity and also OH radicals' availability. The 95% degradation of methylene blue on 20 wt% ZnCdS/MCM-41 is observed within 60 min and it is 46.5% for ZnCdS nanoparticles.

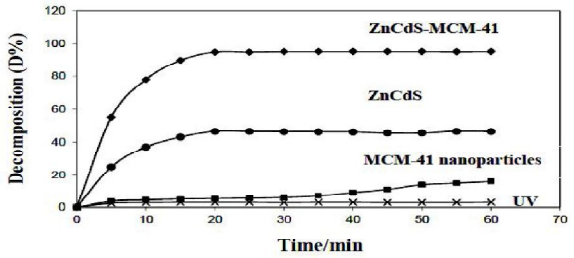


Fig. 5 Effect of UV light and different photocatalyst on photocatalytic degradation of methylene blue. Co = 0.32 ppm, [20 wt% ZnCdS/MCM-41] = 0.4 g/L, pH = 10.

The adsorption capacity of MCM-41 mesoporous enhances the change of OH radicals attack on the adsorbed methylene blue molecules resulting faster degradation rates. Furthermore, ZnCdS nanoparticles dispersion over MCM-41 mesoporous avoids particle-particle aggregation and light scattering by ZnCdS. Apart from all, the delocalizing capacity of MCM-41 mesoporous can effectively separate the electrons and holes produced during photo excitation of ZnCdS, thus enhancing the photocatalytic efficiency [5].

3.3. Effect of variables influence on degradation efficiency

3.3.1. Effect of nanocatalyst amount

In order to determine the optimal amount of photocatalyst, some experiments were performed at pH 10 by varying the amount of catalyst from 0.1 to 6 g/L. The effect of catalyst mount on the rate of degradation is shown in Fig. 6. As seen, the optimum nanocatalyst amount for degradation of basic dye is 0.4 g/L. It is observed that rate increases with increase in catalyst amount from 0.1 to 6 g/L. This is probably due to increase in the number of ZnCdS nanoparticles, that increases the number of photon absorbed and dye molecule absorbed. Increase of the catalyst amount more than 0.4 g/L results in the decrease of degradation rate. This phenomenon may be explained by aggregation of ZnCdS nanoparticles at high concentrations causing a decrease in the number of surface active sites and increase in opacity and light scattering of ZnCdS nanoparticles at high concentration loading to decrease in the passage of irradiation through the sample.

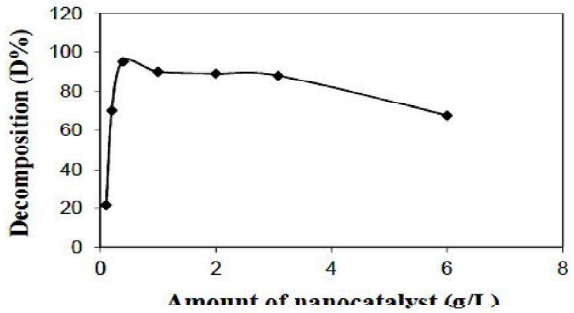


Fig. 6 Change in decomposition% of aqueous solution of methylene blue as a function of catalyst concentration: pH = 10, Co = 0.32 ppm.

3.3.2. Effect of concentration of dyes

The degradation efficiency of dye decreased with increasing the initial concentration of dye to more than 0.32 ppm. The results are shown in Fig. 7. The decrease of %D with increase of concentration of dye can be due to two reasons. With increasing the amounts of dye, the more of dye molecules will be adsorbed on the surface of the photocatalyst and the active sites of the catalysts will be reduced. Therefore, with increasing occupied space of catalyst surface, the generation of hydroxyl radicals will be decreased. Also, increasing concentration of dye can be lead to decreasing the number of photons that is arrived to the surface of catalysts. The more light are adsorbed by molecules of dye and the excition of photocatalyst particles by photons will be reduced. Thus, photodegradation efficiency diminished.

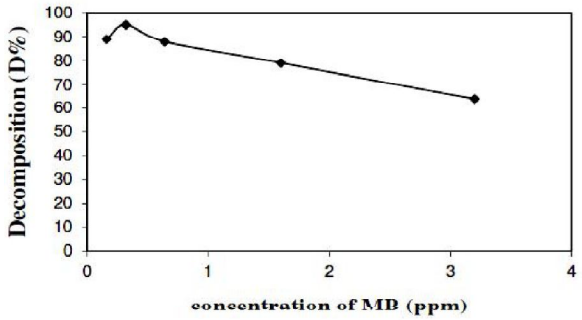


Fig. 7 Effect of concentration of dye on the photodegradation efficiency of methylene blue by ZnCdS/MCM-41 catalyst.

CONCLUSIONS

The nanocomposite semiconductor ZnCdS/MCM-41 nanocrystal, synthesized in present study by ionexchange method, exhibits a superior photocatalytic activity for the destruction of methylene blue under UV light irradiation, and is quite stable under repeated use. The photodegradation conversion of methylene blue decreases with an increase in the initial concentration of methylene blue. One of the main effecting factors is pH and the optimum pH was obtained about 10. The kinetics of photocatalytic degradation of basic blue 9 is of the pseudo-first order with k= 0.034.

ACKNOWLEDGMENTS

Financial support by Rasht Branch, Islamic Azad University Grant No. 4.5830 is gratefully acknowledged.

REFERENCES

[1] M. Rodell, I. Velicogna, and J. S. Famiglietti, “Satellite-based estimates of groundwater depletion in India”, Nature, vol. 460, pp. 999–1002, 2009.

[2] L. Carlsen, R. Bruggemann, Y. Sailaukhanuly, “Application of selected partial order tools to analyze fate and toxicity indicators of environmentally hazardous chemicals”, Ecological Indicators, vol. 29, pp. 191-202, 2013.

[3] M. Heikkinen, H. Poutiainen, M. Liukkonen, T. Heikkinen, Y. Hiltunen, "Subtraction analysis based on self organizing maps for an industrial wastewater treatment process" Math Comput Simulat., vol. 82, pp. 450-459, 2011.

[4] A. Pourahmad, "Photocatalytic Activity of Quantum dots Incorporated in Molecular Sieves for Generation of Hydrogen", Spectrochimica Acta Part A: Molecular and Biomolecular Spectroscopy, vol. 94, pp. 18-22, August 2012.

[5] A. Pourahmad, Sh. Sohrabnezhad, "Preparation and characterization of Ag nanowires in mesoporous MCM-41 nanoparticles template by chemical reduction method", Journal of Alloys and Compounds, vol. 484 no. (1-2), September 2009.

[6] Sh. Sohrabnezhad, A. Pourahmad, M.A. Sadjadi, M.A. Zanjanchi, "Growth and characterization of NiS and NiCoS nanoparticles in mordenite zeolite host", Materials Science and Engineering C, vol. 28, no. 1, January 2008.

[7] H. Wellmann, J. Rathousky, M. Wark, A. Zukal and G. Schulz-Ekloff, "Structural investigation of Zinc Oxide clustering in zeolite A and sodalite", Micropor. Mesopor Mater., vol.44, pp. 419-425, 2001.

[8] W. Chen, Z. Wang, L. Lin, "Thermoluminescence of CdS clusters in zeolite-Y", J. Luminescence., vol.71, pp. 151-156,1997.

★★★